

Dimensionality of superconductivity and vortex dynamics in the infinite-layer cuprate $\text{Sr}_{0.9}\text{M}_{0.1}\text{CuO}_2$ ($\text{M}=\text{La}, \text{Gd}$)

V. S. Zapf,^{1,2} N.-C. Yeh,¹ A. D. Beyer,¹ C. R. Hughes,¹ C. H. Mielke,² N. Harrison,² M. S. Park,³ K. H. Kim,³ and S.-I. Lee³

¹*Department of Physics, California Institute of Technology, Pasadena, California, USA*

²*National High Magnetic Field Laboratory, Los Alamos, New Mexico 87545, USA*

³*Department of Physics, Pohang University of Science and Technology, Pohang, Korea*

(Received 21 April 2004; revised manuscript received 9 December 2004; published 29 April 2005)

The high magnetic-field phase diagram of the electron-doped infinite layer high-temperature superconducting (high- T_c) compound $\text{Sr}_{0.9}\text{La}_{0.1}\text{CuO}_2$ was probed by means of penetration depth and magnetization measurements in pulsed fields to 60 T. An anisotropy ratio of 8 was detected for the upper critical fields with H parallel (H_{c2}^{ab}) and perpendicular (H_{c2}^c) to the CuO_2 planes, with H_{c2}^{ab} extrapolating to near the Pauli paramagnetic limit of 160 T. The longer superconducting coherence length than the lattice constant along the c axis indicates that the orbital degrees of freedom of the pairing wave function are three dimensional. By contrast, low-field magnetization and specific heat measurements of $\text{Sr}_{0.9}\text{Gd}_{0.1}\text{CuO}_2$ indicate a coexistence of bulk s -wave superconductivity with large moment Gd paramagnetism close to the CuO_2 planes, suggesting a strong confinement of the spin degrees of freedom of the Cooper pair to the CuO_2 planes. The region of the magnetic field-temperature phase diagram between H_{c2}^{ab} and the irreversibility line in the magnetization, H_{irr}^{ab} , in $\text{Sr}_{0.9}\text{La}_{0.1}\text{CuO}_2$ is anomalously large for an electron-doped high- T_c cuprate. The large reversible region even approaching zero temperature rules out thermal depinning scenarios. The temperature dependence of H_{irr}^{ab} also differs fundamentally from those predicted for the quenched-disorder-induced vortex phase transitions for $H\parallel c$ at low temperatures. Thus, our finding of a strongly suppressed H_{irr}^{ab} relative to H_{c2}^{ab} at low temperatures is suggestive of the existence of additional quantum fluctuations, possibly due to a magnetic-field-induced competing order such as the spin-density wave (SDW).

DOI: 10.1103/PhysRevB.71.134526

PACS number(s): 74.25.Dw, 74.25.Op, 74.72.Dn, 74.25.Ha

I. INTRODUCTION

In the high- T_c cuprate superconductors, it has been suggested that anisotropy plays an important role in the superconducting pairing mechanism and the elevated T_c in both experimental and theoretical work.^{1,2} It is surprising therefore to find superconductivity (SC) with $T_c=43$ K in the optimal electron-doped infinite-layer cuprates $\text{Sr}_{0.9}\text{M}_{0.1}\text{CuO}_2$ ($\text{M}=\text{La}, \text{Gd}$), which exhibit only a 16% difference between the a and c tetragonal lattice parameters. The structure of $\text{Sr}_{0.9}\text{M}_{0.1}\text{CuO}_2$ is the most basic among all high- T_c cuprates, consisting entirely of CuO_2 sheets separated by rare-earth (RE) ions with tetragonal lattice parameters $c=3.41$ Å and $a=3.95$ Å.³ The recent success in producing high-quality polycrystalline samples of the infinite-layer cuprates with no observable impurity phases³ has engendered a renewed interest in these compounds. X-ray near-edge absorption spectroscopy indicate electron doping,⁴ and bulk SC has been verified by powdered magnetization (M) measurements⁵ and specific heat (C) measurements (data presented later in this work). Several recent studies of these high-purity polycrystalline samples suggest three-dimensional (3D) superconductivity in $\text{Sr}_{0.9}\text{La}_{0.1}\text{CuO}_2$. Scanning tunnel spectroscopy (STS) measurements⁶ indicate an unconventional but isotropic s -wave superconducting gap with no pseudogap at zero field. The s -wave symmetry of the gap is also supported by specific-heat measurements and Cu-site substitution studies,⁶⁻⁸ although it may be contradicted by NMR measurements.⁹ Kim *et al.*⁵ estimated the c -axis coherence

length (ξ_c) from a Hao-Clem analysis¹⁰ of the reversible magnetization of grain-aligned polycrystal and found that ξ_c exceeds the spacing between the CuO_2 planes, indicating 3D superconductivity. On the other hand, they also find significant anisotropy between magnetic fields $H\leq 5$ T oriented parallel and perpendicular to the CuO_2 planes, with an anisotropy ratio $\gamma=\xi_c/\xi_{ab}=H_{c2}^{ab}/H_{c2}^c=9.3$, which is larger than $\gamma=5$ observed in $\text{YBa}_2\text{Cu}_3\text{O}_{7-\delta}$ but much smaller than $\gamma=55$ observed in optimally doped $\text{Bi}_2\text{Sr}_2\text{CaCu}_2\text{O}_{8-\delta}$.^{5,11-13} It is interesting to note that the only major crystallographic difference between the a - b and the c directions in $\text{Sr}_{0.9}\text{La}_{0.1}\text{CuO}_2$ is the presence of oxygen in the a - b plane, which allows coupling of adjacent Cu spins and has been implicated as the cause of antiferromagnetic ordering or spin fluctuations in other members of the high- T_c cuprate family, as well as a possible mechanism for superconducting pairing. The importance of the CuO_2 planes to the SC in $\text{Sr}_{0.9}\text{M}_{0.1}\text{CuO}_2$ is further supported by the fact that Ni substitution on the Cu site rapidly suppresses T_c , whereas out-of-plane Gd substitution on the Sr site leaves T_c unchanged.^{7,14}

In this work we determine the upper critical field H_{c2} and the irreversibility field H_{irr} of $\text{Sr}_{0.9}\text{La}_{0.1}\text{CuO}_2$ by means of magnetization and penetration depth measurements in pulsed magnetic fields up to 60 T in order to directly investigate the degree of upper critical field anisotropy and the role of vortex fluctuations. We also present specific heat (C) and magnetization (M) measurements in low dc fields to 6 T as a function of temperature (T) of $\text{Sr}_{0.9}\text{Gd}_{0.1}\text{CuO}_2$, confirming the bulk coexistence of Gd paramagnetism (PM) and SC.

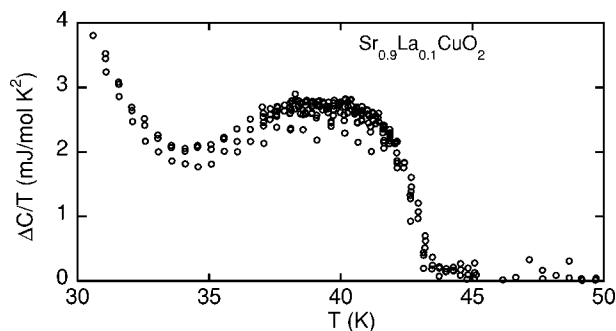


FIG. 1. Specific heat divided by temperature, C/T , vs T at $H=0$ minus C/T at $H=14$ T of polycrystalline $\text{Sr}_{0.9}\text{La}_{0.1}\text{CuO}_2$ showing the superconducting transition.

Our results suggest strong confinement of the spin-pairing wave function to the CuO_2 planes and significant field-induced superconducting fluctuations.

II. EXPERIMENTAL METHODS

Polycrystalline samples of $\text{Sr}_{0.9}\text{La}_{0.1}\text{CuO}_2$ and $\text{Sr}_{0.9}\text{Gd}_{0.1}\text{CuO}_2$ were grown under high pressures as described previously, and c -axis grain-aligned samples of $\text{Sr}_{0.9}\text{La}_{0.1}\text{CuO}_2$ were prepared by mixing powdered polycrystalline compound with epoxy and exposing them to a 11 T magnetic field.^{3,5} Magnetization measurements in pulsed magnetic fields were performed at the National High Magnetic Field Laboratory (NHMFL) in Los Alamos, NM, in a ^3He refrigerator in a 50 T magnet using a compensated coil. The sample consisted of four pieces of polycrystalline $\text{Sr}_{0.9}\text{La}_{0.1}\text{CuO}_2$ with a total mass of 4.8 mg to maximize signal and minimize heating. The irreversibility field H_{irr} was identified from the onset of reversibility in the $M(H)$ loops. The penetration depth of $\text{Sr}_{0.9}\text{La}_{0.1}\text{CuO}_2$ was determined by measuring the frequency shift Δf of a tunnel diode oscillator (TDO) resonant tank circuit with the sample contained in one of the component inductors.¹⁵ A ten-turn 0.7 mm diam aluminum coil was tightly wound around the sample with a filling factor of greater than 90%, with the coil axis oriented perpendicular to the pulsed field. For bulk samples, small changes in the resonant frequency can be related to changes in the penetration depth $\Delta\lambda$ by $\Delta\lambda = -[(R^2/r_s)(\Delta f/f_0)]$, where R is the radius of the coil and r_s is the radius of the sample.¹⁵ In our case, $R \sim r_s = 0.7$ mm and the reference frequency $f_0 \sim 60$ MHz such that $\Delta f \sim (0.16 \text{ MHz}/\mu\text{m})\Delta\lambda$.

III. RESULTS AND ANALYSIS

A. Studies of $\text{Sr}_{0.9}\text{La}_{0.1}\text{CuO}_2$

The bulk nature of superconductivity in $\text{Sr}_{0.9}\text{La}_{0.1}\text{CuO}_2$ is confirmed by specific-heat measurements shown in Fig. 1. The ratio $\Delta C/\gamma T_c = 2.2$ assuming $\gamma = 1.2 \text{ mJ/mol K}^2$.

The frequency shift Δf relative to the normal state and the corresponding $\Delta\lambda$ of bulk randomly oriented polycrystalline $\text{Sr}_{0.9}\text{La}_{0.1}\text{CuO}_2$ are shown in Fig. 2(a) as a function of H . The inset shows the T dependence of Δf in zero magnetic field. The normal-state resonant frequency f that is reached with

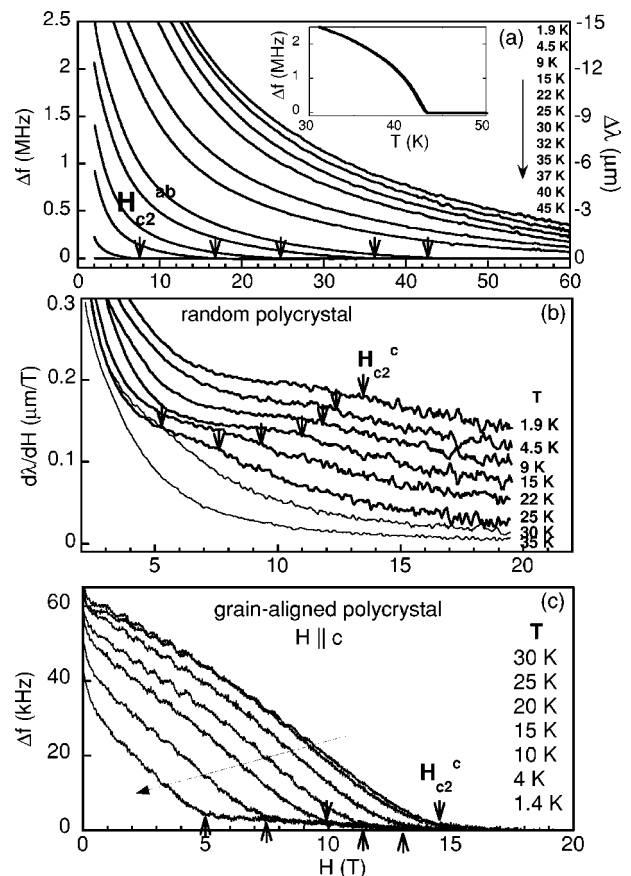


FIG. 2. (a) Change in resonant frequency Δf of the TDO tank circuit relative to the normal state as a function of magnetic field H of a $\text{Sr}_{0.9}\text{La}_{0.1}\text{CuO}_2$ polycrystal at various temperatures T . The estimated change in penetration depth λ is indicated on the right axis. Inset: Δf as a function of T at zero field, where $T_c = 43$ K. (b) Derivative of λ with H for various T , with arrows indicating the kink corresponding to H_{c2} . (c) Δf vs H for c -axis-aligned $\text{Sr}_{0.9}\text{La}_{0.1}\text{CuO}_2$ with H parallel to c for various temperatures.

increasing field can only be determined for $T \geq 30$ K; for lower T the sample remains superconducting to 60 T so Δf is estimated by extrapolation. The frequency shift of the empty coil has been subtracted from all data. The onset of diamagnetism with decreasing H in the $\lambda(H)$ data can be identified with the largest H_{c2} , H_{c2}^{ab} for fields in the CuO_2 planes. The onset is defined as H where $\Delta f > 5$ kHz ($\Delta\lambda > 30$ nm), just above the noise of the experiment. Different onset criteria have only minor effects on the determination of H_{c2}^{ab} , as shown in Fig. 3, where H_{c2}^{ab} using an onset criteria of 5 and 10 kHz are shown as filled circles and diamonds, respectively. This identification of H_{c2}^{ab} is independently confirmed by measurements of c -axis grain-aligned samples with H in the a - b plane, shown as open circles in Fig. 3.

Determination of the critical fields for H along the c axis, H_{c2}^c , has been performed using both polycrystalline samples and c -axis-aligned samples with H parallel to c . For the polycrystalline samples, a change in slope is observed in $\lambda(H)$, indicated as H_{c2}^c in Fig. 2(b). This change in slope would be expected at the lower upper critical field, H_{c2}^c , since the number of grains in the polycrystal that are superconducting var-

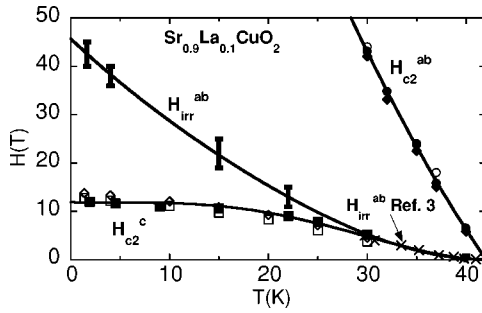


FIG. 3. Field H vs temperature T phase diagram of $\text{Sr}_{0.9}\text{La}_{0.1}\text{CuO}_2$. H_{c2}^{ab} is determined from TDO measurements of polycrystals where Δf exceeds 5 kHz (filled circles) or 10 kHz (filled diamonds), and from c -axis aligned samples where Δf exceeds 2 kHz (open circles). H_{irr}^{ab} : onset of irreversibility in pulsed field M vs H measurements of polycrystals. H_{c2}^c is determined from change in slope of $\lambda(H)$ in TDO measurements of polycrystals (filled squares) or onset of superconductivity in c -axis-aligned samples with 2 kHz onset (open squares) or 5 kHz onset (open diamonds). Crosses indicate onset of irreversibility in M vs T measurements by Jung *et al.*³ Lines are guides to the eye.

ies with H for $H_{c2}^c < H < H_{c2}^{ab}$, whereas for $H < H_{c2}^c$ the entire sample is superconducting, yielding different H dependencies of the flux expulsion in these two regions. This method has been used to extract the anisotropic upper critical fields from magnetization data on randomly aligned powders or polycrystals of MgB_2 and heavy-fermion superconductors by Bud'ko *et al.*¹⁶ Our identification of H_{c2}^c is supported by measurements of c -axis-aligned samples oriented with H parallel to c . The frequency shift as a function of field for the c -axis-aligned samples is shown in Fig. 2(c), and the upper critical field determined from a 2 and 5 kHz onset criteria are indicated in Fig. 3, where again the onset criteria have been chosen to be just above the noise level of the experiment. The determination of H_{c2}^c from the randomly oriented polycrystalline samples is expected to be more accurate because there are no errors in sample or grain alignment.

The $H_{c2}^c(T)$ curve extrapolates to 12 T at $T=0$, close to $H_{c2}^c=14$ T determined from a Hao-Clem analysis mentioned previously.⁵ Our data yield an anisotropy ratio $\gamma=(dH_{c2}^{ab}/dT)/(dH_{c2}^c/dT)\sim 8$, roughly in agreement with $\gamma=9.3$ determined from low field studies.⁵

The irreversibility field of $\text{Sr}_{0.9}\text{La}_{0.1}\text{CuO}_2$ was determined from measurements of magnetization M versus H of polycrystalline $\text{Sr}_{0.9}\text{La}_{0.1}\text{CuO}_2$ in pulsed fields. Following similar arguments for the $\lambda(H)$ measurements, we note that $H_{irr}^{ab} > H_{c2}^c$ in cuprate superconductors, therefore, we assign the onset of irreversibility for polycrystalline $\text{Sr}_{0.9}\text{La}_{0.1}\text{CuO}_2$ to H_{irr}^{ab} . The H_{irr}^{ab} versus T data are shown in Fig. 3, in addition to H_{irr}^{ab} data determined from low-field zero-field-cooled and field-cooled magnetization measurements in a SQUID magnetometer by Jung *et al.*³ The region between H_{irr}^{ab} and H_{c2}^c in the phase diagram is significantly larger than is observed in other electron-doped high- T_c compounds where H_{c2} typically tracks H_{irr} .^{2,17} It is particularly surprising that $H_{irr}^{ab}(T\rightarrow 0)\sim 45$ T is much smaller than $H_{c2}^{ab}(T\rightarrow 0)\sim 150$ T. A large separation between H_{irr} and H_{c2} at moderate to high temperatures is often observed in hole-doped cuprates and is gener-

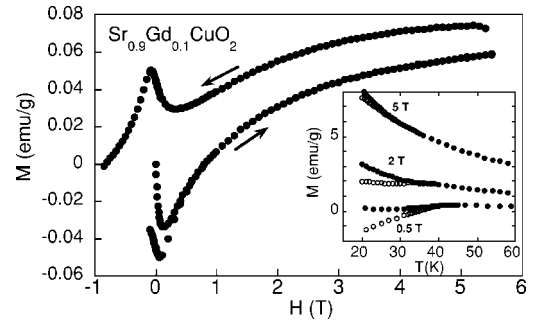


FIG. 4. Magnetization M vs H of polycrystalline $\text{Sr}_{0.9}\text{Gd}_{0.1}\text{CuO}_2$ at $T=5$ K. Inset shows field-cooled (closed symbols) and zero-field-cooled (open symbols) M vs T data at $H=5$, 2, and 0.5 T.

ally referred to as a vortex-liquid phase because of thermally induced fluctuations. However, the large discrepancy between H_{irr}^{ab} and H_{c2}^{ab} in $\text{Sr}_{0.9}\text{La}_{0.1}\text{CuO}_2$ even to $T\rightarrow 0$ cannot be explained by invoking thermal fluctuations. A theory describing a vortex phase transition at zero T as a result of increasing H is necessary. One possibility that warrants further theoretical investigation is the presence of quantum fluctuations as a result of magnetic field-induced competing orders in the cuprate superconductors.¹⁸ Recent neutron-scattering measurements have demonstrated SC coexisting with spin fluctuations or a spin-density wave (SDW) in several high- T_c cuprates.^{19–23} The coexistence of SC and SDW near a quantum critical point has been investigated theoretically as well,¹⁸ and in particular it has been shown that antiferromagnetic spin fluctuations associated with the competing SDW can be enhanced by external fields.^{18,24,25} The conjecture of a competing order in the SC state of $\text{Sr}_{0.9}\text{La}_{0.1}\text{CuO}_2$ is also consistent with our recent STS studies,^{26,27} where we observe the emergence of a second energy gap with increasing tunneling current upon the closing of the SC gap. In contrast to the SC gap, the current-induced gap is not spatially uniform probably due to interactions of the SDW with charge disorder.^{26,27} Neutron-scattering measurements would be necessary to confirm the hypothesis of a coexisting SDW with SC in $\text{Sr}_{0.9}\text{La}_{0.1}\text{CuO}_2$.

B. Studies of $\text{Sr}_{0.9}\text{Gd}_{0.1}\text{CuO}_2$

To elucidate the spin degrees of freedom in the infinite-layer cuprate superconductors, we investigated polycrystalline $\text{Sr}_{0.9}\text{Gd}_{0.1}\text{CuO}_2$ at low fields by means of specific-heat and magnetization measurements. In contrast to in-plane Ni substitution on the Cu site, out of plane Gd substitution on the Sr site does not suppress T_c . In fact, the Gd ions exhibit local moment paramagnetism (PM) that coexists with SC to low T .¹⁴ Figure 4 shows $M(H)$ at $T=5$ K, and zero-field-cooled and field-cooled magnetization curves as a function of T in the inset. The $M(H)$ curve in the main figure can be viewed as a superposition of a SC hysteresis curve and a Brillouin function resulting from the PM of Gd. Further proof for this coexistence is evident in the inset, which shows a large positive magnetization associated with Gd paramagnetism, but nevertheless significant hysteresis be-

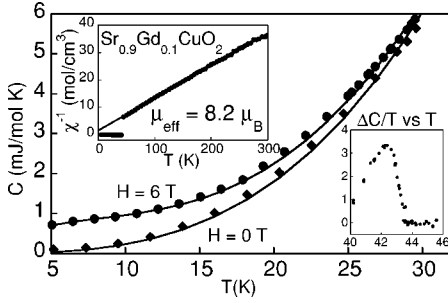


FIG. 5. Main figure: specific heat C vs T at $H=0$ and 6 T. Lines are fits to a field-independent T^3 phonon term plus a contribution from Gd paramagnetism, assuming a Gd total momentum of $J=7/2$. Upper inset: inverse magnetic susceptibility $1/\chi$ vs T with $H=100$ Oe, fit by a Curie-Weiss law above $T_c=43$ K with $\mu_{\text{eff}}=8.2\mu_B$ and $\theta_{CW}=-27$ K. Lower inset: electronic specific heat ΔC vs T showing the superconducting transition.

tween zero-field-cooled and field-cooled curves, indicating superconductivity.

In Fig. 5, the magnitude of the paramagnetic contribution from the Gd ions is investigated quantitatively. The main figure shows $C(T)$ at $H=0$ and $H=6$ T. The $H=0$ data is fit by a T^3 dependence to model the phonon contribution, (the electronic contribution at these temperatures can be neglected). For $H=6$ T, $C(T)$ can be fit by the same T^3 dependence as the $H=0$ data, plus an additional contribution from the Gd paramagnetic moments, derived from mean-field theory assuming the Hund's rule $J=7/2$ moment, and one Gd ion for every ten unit cells. The fit is remarkable, considering that there are no fitting parameters. In the upper inset of Fig. 5, $1/\chi$ is plotted as function of T , where the line is a Curie-Weiss fit with $\mu_{\text{eff}}=8.2\mu_B$, which is close to the Hund's rule moment of $7.6\mu_B$ and the typically observed Gd moment of $8\mu_B$. Thus, we can conclude that all of the Gd ions in the sample are paramagnetic and coexist with SC down to 1.8 K. The bulk nature of the SC in $\text{Sr}_{0.9}\text{Gd}_{0.1}\text{CuO}_2$ is also evident from specific-heat measurements as shown in the lower inset of Fig. 5, which shows the electronic contribution to C plotted as $\Delta C/T$ versus T . ΔC is determined by subtracting the specific heat at $H=1$ T from the zero-field data. The Gd contribution to the specific heat is negligible at these high temperatures. The peak near 43 K is associated with T_c , and the ratio $\Delta C/\gamma T_c$ is 2.9, close to that of $\text{Sr}_{0.9}\text{La}_{0.1}\text{CuO}_2$ mentioned previously, also assuming a Sommerfeld coefficient⁸ of $\gamma=1.2$ mJ/mol K².

IV. DISCUSSION

The coexistence of large-moment Gd ions with bulk superconductivity in $\text{Sr}_{0.9}\text{Gd}_{0.1}\text{CuO}_2$ is surprising since $\text{Sr}_{0.9}\text{Gd}_{0.1}\text{CuO}_2$ is a three-dimensional (3D) s -wave superconductor with a c -axis orbital coherence length $\xi_c=5.2$ Å exceeding both the c -axis lattice parameter c and the distance between the CuO_2 planes and the Gd ions (1.7 Å).⁶ This is in contrast to $\text{Gd}_x\text{Y}_{1-x}\text{Ba}_2\text{Cu}_3\text{O}_7$, where SC and Gd paramagnetism also coexist with ξ_c greater than the CuO_2 -Gd spacing,^{28,29} however, the symmetry of the superconducting wave function is generally believed to be d wave and the

superconductivity is two-dimensional (2D) in nature ($\xi_c < c$). In $\text{Sr}_{0.9}\text{Gd}_{0.1}\text{CuO}_2$, the apparent problem of 3D isotropic s -wave SC coexisting with strong Gd local moments less than 1.7 Å from the CuO_2 planes can be resolved by considering different length scales for orbital and spin interactions among Cooper pairs. The coherence length ξ_c derived from BCS and Ginzburg-Landau theories of superconductivity describes the spatial extent of the orbital wave function of the Cooper pairs and is not necessarily related to the spin-spin interaction distance. In the cuprates, the superexchange coupling between adjacent Cu spins in the CuO_2 plane is thought to be mediated by the O atoms and is therefore highly directional along the Cu–O bonds. Thus the spin and orbital parts of the superconducting wave function can be considered separately, with the orbital wave function overlapping adjacent CuO_2 planes producing 3D superconductivity, whereas the spin-wave function is strongly confined to the CuO_2 planes.

Finally, we compare our proposed scenario of field-induced quantum fluctuations for a strongly suppressed H_{irr}^{ab} with a recent theoretical study³⁰ that investigated the effect of quenched disorder and thermal fluctuations on the vortex dynamics of anisotropic type-II superconductors. In the work by Kierfeld and Vinokur,³⁰ it is found that quenched disorder can lead to an order-to-disorder vortex phase transition for $H\parallel\hat{c}$ in the cuprate superconductors, and the phase boundary that separates the low-field Bragg glass (BrG) from the high-field vortex glass (VG) is nearly independent of T for temperatures below the depinning temperature.³⁰ On the other hand, at sufficiently high fields, a vortex-glass-to-vortex-liquid (VL) melting transition can take place with increasing temperature, and the VG-to-VL phase boundary exhibits a strong temperature dependence, which extends to H_{c2}^{Hc} for $T\rightarrow 0$.³⁰ Clearly neither the VG-to-VL nor the BrG-to-VG phase transition line agrees with the temperature dependence of the H_{irr}^{ab} line of our $\text{Sr}_{0.9}\text{La}_{0.1}\text{CuO}_2$ sample. The order-to-disorder vortex phase transition is expected to be nearly temperature independent, in contrast with our results. In addition, as mentioned in Sec. III, the vortex configuration associated with $H\parallel ab$ in the cuprate superconductors is the least sensitive to disorder-induced fluctuations because of strong intrinsic confinement of vortices by the periodic CuO_2 layered structure. In particular, this intrinsic confinement is expected to be the strongest for the infinite-layer cuprates because the c -axis lattice constant is identical to the distance between two consecutive CuO_2 layers. A thermal-fluctuation-induced depinning scenario can also be ruled out since the depinning effects observed in $\text{Sr}_{0.9}\text{La}_{0.1}\text{CuO}_2$ remain significant as $T\rightarrow 0$. In a purely thermal depinning scenario, the irreversibility field should approach H_{c2} as $T\rightarrow 0$. Thus an additional mechanism for vortex depinning is necessary to explain the phase diagram for $\text{Sr}_{0.9}\text{La}_{0.1}\text{CuO}_2$. Recent theoretical^{18,24,25} and experimental^{19–23,26,27} studies for cuprate superconductors have shown that competing orders in the cuprates may be induced by either increasing magnetic field or increasing temperature, and the induced competing order may be further stabilized by disorder. We therefore conjecture that the presence of competing order can affect the vortex dynamics of the cuprate superconductors in a fundamental way. This issue awaits future theoretical investigation.

V. SUMMARY

In conclusion, a large upper critical field anisotropy ratio $\gamma=8$ has been inferred from penetration depth measurements of $\text{Sr}_{0.9}\text{La}_{0.1}\text{CuO}_2$ in pulsed fields, despite the nearly cubic crystal structure. The in-plane upper critical field H_{c2}^{ab} extrapolates close to the Pauli paramagnetic limit $H_{c2}^P=159$ T, suggesting possible spin-limiting superconductivity for this orientation, as has been observed in $\text{YBa}_2\text{Cu}_3\text{O}_{7-\delta}$.³¹ There is a large separation between H_{c2}^{ab} and the irreversibility field H_{irr}^{ab} , which extends down to $T \rightarrow 0$, suggesting the existence of field-induced quantum fluctuations perhaps because of a competing SDW. In spite of the significant anisotropy in the upper critical fields, ξ_c , is longer than the spacing between CuO_2 planes, indicating three-dimensionality of the orbital wave function. The low-field measurements of $\text{Sr}_{0.9}\text{Gd}_{0.1}\text{CuO}_2$ polycrystals indicate a coexistence of bulk

SC with Gd paramagnetism, with the full $J=7/2$ Hund's rule moment despite the close proximity of Gd atoms to the CuO_2 planes, and a T_c of 43 K in both $\text{Sr}_{0.9}\text{Gd}_{0.1}\text{CuO}_2$ and $\text{Sr}_{0.9}\text{La}_{0.1}\text{CuO}_2$. This can be interpreted in terms of a strong confinement of the spin degrees of freedom of the Cooper pairs to the CuO_2 planes, whereas the orbital wave functions overlap adjacent CuO_2 planes and exhibit isotropic s -wave symmetry as determined by STS measurements.⁶

ACKNOWLEDGMENTS

This work was supported by the National Science Foundation under Grant No. DMR-0103045 and DMR-0405088, and through the National High Magnetic Field Laboratory. V.Z. acknowledges support from the Caltech Millikan Postdoctoral Fellowship program and the Department of Energy through the LANL Director-Funded Postdoctoral program.

- ¹See, e.g., P. W. Anderson, *The Theory of Superconductivity in High- T_c Cuprates* (Princeton University Press, Princeton, NJ, 1997), and references therein.
- ²M. B. Maple, E. D. Bauer, V. S. Zapf, and J. Wosnitzer, in *The Physics of Superconductors*, edited by K. H. Bennemann and J. B. Ketterson (Springer, 2004), Vol. II, Chap. 8, pp. 555–730.
- ³C. U. Jung, J. Y. Kim, M.-S. Kim, M.-S. Park, H.-J. Kim, Y. Yao, S. Y. Lee, and S.-I. Lee, *Physica C* **366**, 299 (2002).
- ⁴R. S. Liu, J. M. Chen, P. Nachimuthu, R. Gundakaram, C. U. Jung, J. Y. Kim, and S. I. Lee, *Solid State Commun.* **118**, 367 (2001).
- ⁵M.-S. Kim, T. R. Lemberger, C. U. Jung, J.-H. Choi, J. Y. Kim, H.-J. Kim, and S.-I. Lee, *Phys. Rev. B* **66**, 214509 (2002).
- ⁶C.-T. Chen, P. Seneor, N.-C. Yeh, R. P. Vasquez, L. D. Bell, C. U. Jung, J. Y. Kim, M.-S. Park, H.-J. Kim, and S.-I. Lee, *Phys. Rev. Lett.* **88**, 227002 (2002).
- ⁷C. U. Jung, J. Y. Kim, M.-S. Park, M.-S. Kim, H.-J. Kim, S. Y. Lee, and S.-I. Lee, *Phys. Rev. B* **65**, 172501 (2002).
- ⁸Z. Y. Liu, H. H. Wen, L. Shan, H. P. Yang, X. F. Lu, H. Gao, M.-S. Park, C. U. Jung, and S.-I. Lee, *Europhys. Lett.* **69**, 263 (2005).
- ⁹G. V. M. Williams, R. Dupree, A. Howes, S. Kramer, H. J. Trodahl, C. U. Jung, M.-S. Park, and S.-I. Lee, *Phys. Rev. B* **65**, 224520 (2002).
- ¹⁰Z. Hao, J. R. Clem, M. W. McElfresh, L. Civale, A. P. Malozemoff, and F. Holtzberg, *Phys. Rev. B* **43**, 2844 (1991).
- ¹¹M.-S. Kim, C. U. Jung, J. Y. Kim, J.-H. Choi, and S.-I. Lee, *Solid State Commun.* **123**, 17 (2002).
- ¹²D. E. Farrell, S. Bonham, J. Foster, Y. C. Chang, P. Z. Jiang, K. G. Vandervoort, D. J. Lam, and V. G. Kogan, *Phys. Rev. Lett.* **63**, 782 (1989).
- ¹³D. E. Farrell, C. M. Williams, S. A. Wolf, N. P. Bansal, and V. G. Kogan, *Phys. Rev. Lett.* **61**, 2805 (1988).
- ¹⁴C. U. Jung, J. Y. Kim, S.-I. Lee, and M.-S. Kim, *Physica C* **391**, 319 (2003).
- ¹⁵C. Mielke, J. Singleton, M.-S. Nam, N. Harrison, C. C. Agosta, B. Fravel, and L. K. Montgomery, *J. Phys.: Condens. Matter* **13**, 8325 (2001).
- ¹⁶S. L. Bud'ko, V. G. Kogan, and P. C. Canfield, *Phys. Rev. B* **64**, 180506(R) (2001).
- ¹⁷P. Fournier and R. L. Greene, *Phys. Rev. B* **68**, 094507 (2003).
- ¹⁸E. Demler, S. Sachdev, and Y. Zhang, *Phys. Rev. Lett.* **87**, 067202 (2001).
- ¹⁹Y. S. Lee, R. J. Birgeneau, M. A. Kastner, Y. Endoh, S. Wakimoto, K. Yamada, R. W. Erwin, S.-H. Lee, and G. Shirane, *Phys. Rev. B* **60**, 3643 (1999).
- ²⁰H. J. Kang, P. Dai, J. W. Lynn, M. Matsuura, J. R. Thompson, S.-C. Zhang, D. N. Argyriou, Y. Onose, and Y. Tokura, *Nature (London)* **423**, 522 (2003).
- ²¹M. Matsuura, P. Dai, H. J. Kang, J. W. Lynn, D. N. Argyriou, K. Prokes, Y. Onose, and Y. Tokura, *Phys. Rev. B* **68**, 144503 (2003).
- ²²B. Lake, H. M. Ronnow, N. B. Christensen, G. Aeppli, K. Lefmann, D. F. McMorrow, P. Vorderwisch, P. Smeibidl, N. Mangkorntong, T. Sasagawa, M. Nohara, H. Takagi, and T. E. Mason, *Nature (London)* **415**, 299 (2002).
- ²³H. A. Mook, P. Dai, S. M. Hayden, A. Hiess, J. W. Lynn, S.-H. Lee, and F. Dogan, *Phys. Rev. B* **66**, 144513 (2002).
- ²⁴S. Sachdev and S. C. Zhang, *Science* **295**, 452 (2002).
- ²⁵C.-T. Chen and N.-C. Yeh, *Phys. Rev. B* **68**, 220505(R) (2003).
- ²⁶N.-C. Yeh, C.-T. Chen, V. S. Zapf, A. D. Beyer, C. R. Hughes, M.-S. Park, K.-H. Kim, and S.-I. Lee, *cond-mat/0408100*, *Int. J. Mod. Phys. B* (to be published).
- ²⁷N. C. Yeh, C.-T. Chen, A. D. Beyer, C. R. Hughes, T. A. Corcovilos, and S.-I. Lee, *Physica C* **408–410**, 792 (2004).
- ²⁸J. M. Tarascon, W. R. McKinnon, L. H. Greene, G. W. Hull, and E. M. Vogel, *Phys. Rev. B* **36**, 226 (1987).
- ²⁹U. Welp, W. K. Kwok, G. W. Crabtree, K. G. Vandervoort, and J. Z. Liu, *Phys. Rev. Lett.* **62**, 1908 (1989).
- ³⁰J. Kierfeld and V. Vinokur, *Phys. Rev. B* **69**, 024501 (2004).
- ³¹J. L. O'Brien, H. Nakagawa, A. S. Dzurak, R. G. Clark, B. E. Kane, N. E. Lumpkin, R. P. Starrett, N. Muir, E. E. Mitchell, J. D. Goettee, D. G. Rickel, and J. S. Brooks, *Phys. Rev. B* **61**, 1584 (2000).